Soils and Rocks

An International Journal of Geotechnical and Geoenvironmental Engineering

www.soilsandrocks.com

ISSN 1980-9743
ISSN-e 2675-5475

Probabilistic framework for characterising analytical model uncertainty in geosynthetic-reinforced soil walls

Marcell Gustavo Chagas Santos[1#], Jefferson Lins da Silva[1], Gabriel da Silva Silverio[1], Bryan Robin Sanchez Ramirez[1]

Technical Note

Keywords
Geosynthetic-reinforced soil wall
Analytical model uncertainty
Bayesian updating
Reliability-based design

Abstract

Quantifying the main sources of uncertainty associated with analytical models for predicting reinforcement loads is essential for ensuring safety, supporting reliability analyses, and enabling reliability-based optimization in geotechnical design. This paper presents a probabilistic framework to characterise uncertainty in load prediction models for geosynthetic-reinforced soil walls. Model uncertainty is assessed through a Bayesian updating framework that compares analytical predictions with monitoring data from well-instrumented walls, while explicitly accounting for the uncertainties associated with model parameter estimation. The random variables considered include the soil unit weight and the angle of internal friction. The applicability of the framework is illustrated using two simple analytical methods: the American Association of State Highway and Transportation Officials (AASHTO) Simplified Method and the *K-Stiffness* Method. This framework also allows model uncertainty to be updated as new monitoring data become available. In addition, it can be extended to other analytical or numerical models commonly employed for the design of geosynthetic-reinforced soil walls. This flexibility enhances its potential for practical adoption and for guiding future reliability-based studies.

1. Introduction

Analytical models are widely used in geotechnical engineering to predict the performance of soil-structure systems. These models are based on assumptions that idealize the behavior of geomaterials, thus simplifying the real behavior. Furthermore, soil is a heterogeneous material with complex and highly variable behavior. As a result, the responses of geotechnical models are inherently approximations. Thus, geotechnical system performance and safety depend strongly on the accuracy of the design models. Consequently, quantifying and incorporating model uncertainty into geotechnical practices is essential for improving reliability.

Model uncertainty can be characterised by a systematic comparison between model predictions and observed performance. However, a direct comparison may be inadequate, since uncertainties in input parameters and measurement data can also contribute to the differences between model predictions and observed performance (Zhang et al., 2009, 2012).

Although the importance of model uncertainty in geotechnical engineering is widely recognized, recent studies addressing this topic remain limited and often focus on specific applications. Khademian et al. (2017) evaluated model uncertainty in settlement prediction for a subway tunnel excavation. Tang & Phoon (2019) assessed uncertainty in driven pile design using 239 static load tests. Heidarie Golafzani et al. (2020) incorporated model uncertainty into reliability-based assessments of axial pile bearing capacity. More recently, Hosseinpour et al. (2024) used a probabilistic site-effect assessment algorithm considering uncertainties in geological models and geotechnical parameters for the development of probabilistic seismic microzonation.

A practical approach for the characterisation and updating of model uncertainty in predicting the behavior of geosynthetic-reinforced soil walls is essential for enhancing safety and supporting the development of reliability-based design. Estimating model uncertainty helps improve the reliability of design predictions, reduce conservatism, and support informed engineering decisions. Furthermore, it enables advances in modern design methodologies (Phoon & Kulhawy, 2005; Dithinde et al., 2011; Belo et al., 2022; Assis & Nogueira, 2023; Hosseinpour et al., 2024), such as reliability-based design optimization approaches, which integrate uncertainty into the decision-making process (Basha & Babu, 2010, 2012; Santos et al., 2018; Mahmood et al., 2022).

[#]Corresponding author. E-mail address: marcell.gustavo@usp.br
[1]Universidade de São Paulo, Escola de Engenharia de São Carlos, Departamento de Geotecnia, São Carlos, SP, Brasil.

Submitted on September 3, 2025; Final Acceptance on January 28, 2026; Discussion open until November 30, 2026.

Editor: Renato P. Cunha

https://doi.org/10.28927/SR.2026.014725

This study presents a practical framework to characterise the model uncertainty associated with analytical methods used to design geosynthetic-reinforced soil walls under static loading. A Bayesian updating framework, originally proposed by Zhang et al. (2009, 2012), is employed to quantify model uncertainty based on the comparison between predicted and measured reinforcement loads in well-instrumented walls. The applicability of the framework is illustrated using two analytical methods: the AASHTO Simplified Method (AASHTO, 2014) and the *K-Stiffness* Method modified by Miyata & Bathurst (2007). The analysis is based on a dataset comprising 80 measured reinforcement loads collected from 17 well-documented geosynthetic-reinforced walls reported in the literature. It should be emphasized that this work does not aim to provide an exhaustive assessment of the uncertainty associated with these analytical models. Instead, the selected design methods and case histories serve to demonstrate the practical implementation of the proposed approach, highlighting its robustness as a tool to support reliability-based design. In practical applications, model uncertainty should be updated by considering prior knowledge and incorporating reliable and representative case histories relevant to the project under consideration.

2. Bayesian framework for characterising model uncertainty

The methodology proposed by Zhang et al. (2009, 2012) enables the characterisation and updating of model uncertainty in geotechnical systems, considering the natural variability of input parameters and the measurement errors in observed performance data. This approach is grounded in the concept of Bayesian updating, whereby prior knowledge about model uncertainty is revised using observed performance data. In this context, observations from similar geotechnical systems can be used to infer model uncertainty, even when the input parameters are uncertain, and the observed response is affected by measurement errors.

Let $g_{(\theta)}$ denote a model used to predict the behavior of a geotechnical system, where θ represents a vector of uncertain input parameters. Due to model uncertainty, $g_{(\theta)}$ may not represent the real response (y) of the system. Thus, a model correction factor (ε) can be introduced to represent the effect of model uncertainty. The model correction factor can be applied additively (Christian et al., 1994; Cetin et al., 2002; Moss et al., 2006; Zhang et al., 2009) or multiplicatively (Gilbert & Tang, 1995; Juang et al., 2004; Zhang et al., 2012). In this study, the additive formulation was adopted, as shown in Equation 1.

$$y = g\left(\theta\right) + \varepsilon \tag{1}$$

The presence of error during the process of measuring the performance of the geotechnical system implies that the observed response (d) may not represent the real response (y). Similar to the model correction factor, an observation uncertainty factor (Δ) is applied, as shown in Equation 2.

$$d = y + \Delta \tag{2}$$

Combining Equations 1 and 2, the relationship between $g_{(\theta)}$, Δ, ε and d is expressed by Equation 3.

$$d = g_{(\theta)} + \Delta + \varepsilon \tag{3}$$

Since the objective is to characterise model uncertainty, we define $G_{(x)} = g_{(\theta)} + \Delta$, where $x = \left\{\theta, \Delta\right\}$. Substituting into Equation 3, we obtain:

$$d = G_{(x)} + \varepsilon \tag{4}$$

For practical studies in geotechnical engineering, it is common to consider a normal distribution to describe a random variable. Thus, it is convenient to assume that ε follows a normal distribution with mean μ_ε and standard deviation σ_ε. Therefore, the probability density function of ε is given by Equation 5.

$$f_{(\varepsilon|\mu_\varepsilon,\sigma_\varepsilon)} = \frac{1}{\sigma_\varepsilon\sqrt{2\pi}}\exp^{\left[-\frac{\left(\varepsilon-\mu_\varepsilon\right)^2}{2\sigma_\varepsilon{}^2}\right]} \tag{5}$$

Based on Equations 4 and 5, d is normally distributed with mean of $G_{(x)} + \mu_\varepsilon$ and standard deviation of σ_ε, if x, μ_ε and σ_ε are known. The conditional probability density function of d given x, μ_ε and σ_ε is given by Equation 6.

$$f_{(d|\mu_\varepsilon,\sigma_\varepsilon,x)} = \frac{1}{\sigma_\varepsilon\sqrt{2\pi}}exp^{\left[-\frac{\left(d_i-G_{(x_i)}-\mu_\varepsilon\right)^2}{2\sigma_\varepsilon{}^2}\right]} \tag{6}$$

Given historical data from n similar geotechnical systems, where both x and d are known, model uncertainty can be characterised. Assuming statistical independence, the likelihood is expressed as the product of the probabilities of individual observations, as shown in Equation 7.

$$L_{(\mu_\varepsilon,\sigma_\varepsilon,X|d)} = \prod_{i=1}^{n}\frac{1}{\sigma_\varepsilon\sqrt{2\pi}}exp^{\left[-\frac{\left(d_i-G_{(x_i)}-\mu_\varepsilon\right)^2}{2\sigma_\varepsilon{}^2}\right]} \tag{7}$$

Here, $X = \left\{x_1, x_2, \ldots, x_n\right\}$ and $d = \left\{d_1, d_2, \ldots, d_n\right\}$. Let $f_{(\mu_\varepsilon,\sigma_\varepsilon)}$ and $f_{(x_i)}$ denote the probability density functions of the prior knowledge of $\left\{\mu_\varepsilon, \sigma_\varepsilon\right\}$ and x_i, respectively. Thus, according to Bayes' theorem, the subsequent probability density function of $\left\{\mu_\varepsilon, \sigma_\varepsilon, X\right\}$ is given by Equation 8.

$$f_{(\mu_\varepsilon,\sigma_\varepsilon,X|d)} = k.f_{(\mu_\varepsilon,\sigma_\varepsilon)}\prod_{i=1}^{n}\frac{1}{\sigma_\varepsilon\sqrt{2\pi}}exp^{\left[-\frac{\left(d_i-G_{(x_i)}-\mu_\varepsilon\right)^2}{2\sigma_\varepsilon{}^2}\right]}.f_{(x_i)} \tag{8}$$

Where k is the normalization constant to make the probability density function valid. As the interest is to estimate the statistics of ε, X in the subsequent distribution can be eliminated by integration. The update of the knowledge of μ_ε and σ_ε can be obtained from Equation 9.

$$f_{(\mu_\varepsilon,\sigma_\varepsilon|d)} = k.f_{(\mu_\varepsilon,\sigma_\varepsilon)}\prod_{i=1}^{n} \int\ldots\int_{s_{(x_i)}}\frac{1}{\sigma_\varepsilon\sqrt{2\pi}}exp^{\left[-\frac{\left(d_i-G_{(x_i)}-\mu_\varepsilon\right)^2}{2\sigma_\varepsilon{}^2}\right]}.f_{(x_i)}\cdot d_{x_i} \tag{9}$$

Where $S_{(x_i)}$ denotes the space of x_i. Equation 9 provides a theoretical framework for characterising the uncertainty of a model when input parameters and observation data are subject to uncertainty. However, this formulation is not practically applicable. The large number of random variables (x_i(i = 1, 2, ..., n), μ_ε and σ_ε), the number of integrations (n) and the complexity of the geotechnical model ($g_{(\theta)}$) make the numerical solution of Equation 9 difficult. To address these computational challenges, Zhang et al. (2009) proposed an approximate solution, as shown in Equation 10.

$$f_{(\mu_\varepsilon,\sigma_\varepsilon|d)} \approx k\cdot f_{(\mu_\varepsilon,\sigma_\varepsilon)} \prod_{i=1}^{n}\frac{1}{\sqrt{2\pi\left(\sigma_\varepsilon{}^2+\sigma_{G(x_i)}{}^2\right)}}\exp\left[-\frac{\left(d_i-\mu_{G(x_i)}-\mu_\varepsilon\right)^2}{2\left(\sigma^2_{\varepsilon^2+\sigma_G(x_i)^2}\right)}\right] \tag{10}$$

In Equation 10, $\mu_{G_{(x_i)}}$ and $\sigma_{G_{(x_i)}}$ are the mean and standard deviation of $G_{(x_i)}$ and can be calculated using Monte Carlo simulation. Thus, Equation 10 involves only two random variables (μ_ε and σ_ε) and eliminates the multiple integrations and complexity of the geotechnical model from the Bayesian framework.

One of the ways to solve Equation 10 is by using the Metropolis-Hastings algorithm, Gelman et al. (2014), which is a rejection sampling algorithm used to generate a sequence of samples from a probability distribution. The posterior statistics of μ_ε and σ_ε can be inferred from the samples generated by the Metropolis-Hastings algorithm.

To solve the original problem of characterising model uncertainty, Equation 8, the Monte Carlo sampling method via Markov chain (MCMC simulation) can be adopted. MCMC simulation is a method for extracting samples from an arbitrary distribution by means of a Markov chain that converges to the target distribution. This approach has been used in geotechnical engineering by Wang et al. (2010), Zhang et al. (2010, 2012) and Santoso et al. (2011).

To solve Equation 8, Zhang et al. (2012) proposed an approach, called Hybrid MCMC Simulation, which combines the Metropolis algorithm, Metropolis et al. (1953), and the Gibbs sampler, Geman & Geman (1984), to generate Markov chains.

In this study, the approximate solution proposed by Zhang et al. (2009) was used to define the prior probability density function of $\{\mu_\varepsilon,\sigma_\varepsilon\}$. The posterior distribution $f_{(\mu_\varepsilon,\sigma_\varepsilon,X|d)}$ was then updated using the Hybrid MCMC methodology developed by Zhang et al. (2012). The Markov chain was constructed using a normal distribution as the jump function.

3. Application of the probabilistic framework to model uncertainty

To characterise the model uncertainty applying the methodologies described by Zhang et al. (2009, 2012), reliable measured data of the studied system are needed. In this study, to assess the uncertainty associated with the AASHTO Simplified Method (AASHTO, 2014) and the *K-stiffness* method (Miyata & Bathurst, 2007), a dataset comprising 80 measured axial reinforcement loads from 17 full-scale geosynthetic-reinforced soil walls with cohesionless backfill, subjected to static surcharge loading and constructed with varying geometries and materials, was analyzed.

The dataset includes measured loads from several well-instrumented walls: GW16 and GW16 with surcharge (Allen et al., 1992), GW9 and GW9 with surcharge (Bathurst et al., 1993), GW5 (Bright et al., 1994), GW20-HDPE and GW20-PP (Carrubba et al., 1999), GW8 and GW10 (Christopher, 1993), GW7–Section J and GW7–Section N (Fannin & Hermann, 1990), GW18 (Knight & Valsangkar, 1993), GW19 (Schlosser et al., 1993), and GW22 to GW25 (Tajiri et al., 1996). The main characteristics of the walls, such as height, face type, inclination, and geotechnical parameters, are summarized in Table 1. For additional details, readers are referred to the original references. The nomenclature used for identifying each wall follows the conventions proposed by Allen et al. (2002) and Miyata & Bathurst (2007). The scope of this study is limited to soil walls reinforced with geosynthetics constructed with granular soil fills (cohesionless soils), considering only internal failure mechanisms under static loading conditions.

It should be noted that these case studies were selected solely to provide an illustrative dataset for applying the probabilistic framework. Therefore, they do not represent an exhaustive review of all available full-scale tests, but rather a representative sample that enables demonstrating the methodology in a practical and transparent way.

In this study, the uncertainty associated with measurement data is unknown. Therefore, for simplicity, the observation uncertainty factor (Δ) is neglected, and the model uncertainty is given by $G(x) = g(\theta)$. However, in practical design applications, the uncertainty associated with measurement data should not be disregarded, as its consideration is essential to ensure greater robustness and reliability in engineering decisions.

To account for the intrinsic soil variability, in each case, the uncertainty vector is composed of the soil unit weight and internal friction angle, $x = \{\theta\} = \{\gamma;\phi\}$.

To determine the model uncertainty using the MCMC simulation approach proposed by Zhang et al. (2012), it is first necessary to define a prior distribution for μ_ε and σ_ε, as well as the uncertainty of γ and ϕ. For the former, initial estimates are obtained using the method presented by Zhang et al. (2009), in which the statistics of $g(x)$ are evaluated through Monte Carlo simulation with 50000 samples. For the latter parameters, prior knowledge was derived from literature sources and engineering judgment (e.g., Lacasse & Nadim, 1996; Duncan, 2000; Ferreira et al., 2016). In this work, the prior distribution of γ was defined as log-normal with a coefficient of variation (*COV*) of 10%, while ϕ was modeled as normal with a *COV* of 7.5%.

A total of 10000 samples were used to evaluate the statistical behavior of μ_ε and σ_ε through the simplified method of Zhang et al. (2009). However, the initial samples of the Markov chain may be unstable; therefore, only the last 5000 samples were considered to determine the statistical parameters. The results are presented in Table 2.

The statistical estimates obtained using the simplified approach by Zhang et al. (2009) were adopted as prior knowledge for the hybrid MCMC simulation proposed by Zhang et al. (2012). Preliminary analyses were then performed to evaluate the influence of the initial point, jump function parameters, and Markov chain length on its performance.

To assess the influence of choice of the initial point, simulations were conducted using both a fixed initial point $\{\mu_\varepsilon^0, \sigma_\varepsilon^0\}$ and randomly generated points within a range approximately three times the mean values obtained from the simplified analysis. The results indicate that variations within this range do not affect the convergence of the algorithm, as differences in μ_ε and σ_ε, when present, were limited to the second decimal place.

Table 1. Summary of walls used in this study.

Wall	Wall height (m)	Face type	Face inclination (°)	Geosynthetic type	γ (kN/m^3)	ϕ (°)
GW5	4.7	Full-height propped concrete panel	90	Extruded geogrid (HDPE)	19.6	53
GW7(1)	4.8	Welded wire facing units	117	Extruded geogrid (HDPE)	17.0	46
GW8	6.1	Incremental concrete panel	90	Extruded geogrid (HDPE)	20.4	43
GW9(2)	6.1	Segmental (masonry block) facing units	93	Woven geogrid (PET)	20.4	43
GW10	5.9	Wrapped-face	90	Nonwoven geotextile (PET)	20.4	43
GW16(2)	12.6	Geotextile wrapped-face	93	Woven geotextile (PP and PET)(3)	21.1	93
GW18	6.1	Full-height propped concrete panel	90	Extruded geogrid (HDPE)	20.4	45
GW19	6.4	Incremental concrete panel	90	Geostrip (PET)	16.4	42
GW20(4)	4.0	Welded wire facing units	95	Extruded geogrid (HDPE and PP)	21.1	57
GW22	6.0	EPS block facing	90	Extruded geogrid (HDPE)	16.7	48
GW23	6.0	Incremental concrete panel	90	Extruded geogrid (HDPE)	16.7	48
GW24	6.0	Full-height propped concrete panel	90	Extruded geogrid (HDPE)	16.7	48
GW25	6.0	Solid masonry block	90	Extruded geogrid (HDPE)	16.7	48

(1)GW7 was designed in two sections (J and N sections) with different reinforcement spacing and length. (2)Walls constructed under both surcharge and non-surcharge conditions. (3)GW16 was divided into zones using woven geotextiles made with different polymers (PP and PET). (4)GW20 was constructed with two section types: one reinforced with a uniaxial HDPE geogrid and the other with a biaxial PP geogrid. HDPE = High-density polyethylene. PET = Polyester. PP = Polypropylene.

Table 2. Previous knowledge of ε .

Design method	Dist.	μ_ε		σ_ε	
		Mean	*SD*	Mean	*SD*
AASHTO	Normal	-4.06	0.49	3.66	0.42
K-stiffness	Normal	-0.06	0.07	0.43	0.07

The results above do not imply that any starting point can be selected. When the initial point deviates significantly from the true model characterisation parameters, a longer Markov chain is required to ensure convergence. Therefore, it is recommended to perform preliminary analyses using the simplified model, with a starting point near the origin, to evaluate the chain's behavior, verify its stabilization, and define an adequate starting point.

The convergence of the algorithm is also influenced by the choice of the jump function parameters used to generate random samples during the construction of the Markov chain. As a preliminary step, analyses were conducted using the simplified model to define suitable jump function parameters. The jump function was modeled assuming normal distributions for both μ_ε and σ_ε. For the AASHTO Simplified Method, a standard deviation of 0.5 was adopted ($SD_{adeq\_\mu_\varepsilon} = SD_{adeq\_\sigma_\varepsilon} = 0.5$), while for the *K-Stiffness* Method a smaller value of 0.1 was used ($SD_{adeq\_\mu_\varepsilon} = SD_{adeq\_\sigma_\varepsilon} = 0.1$). Accordingly, the influence of these parameters on the convergence of the hybrid MCMC algorithm was assessed by varying the standard deviation of the jump function within the range $0.1SD_{adeq} \le SD_{adeq} \le 10SD_{adeq}$. It is well known that adopting a very large standard deviation in the jump function is associated with a low acceptance rate, whereas using a small standard deviation leads to a high acceptance rate. Gelman et al. (2014) suggested that the acceptance rate should be close to 0.44 to produce efficient Markov chains. In this study, low standard deviation values resulted in acceptance rates between 0.88 and 0.94, while high standard deviation values yielded acceptance rates of 0.08 and 0.09. Nevertheless, the results indicate that, regardless of the standard deviation, algorithm convergence was achieved when the Markov chain length was equal to or greater than 10000 samples.

Finally, to investigate the influence of Markov chain length on algorithm convergence, simulations were conducted with different numbers of samples (1000; 3000; 5000; 10000; and 30000). When using a starting point near the true model characterisation parameters and adopting suitable jump function parameters, the results for the statistical values and distributions of $\mu\varepsilon$ and $\sigma\varepsilon$ indicate that 3000 samples are sufficient for the algorithm to converge. Increasing the number of samples (5000; 10000; and 30000) provided further improvements but also led to substantially longer processing times (approximately 1.7, 3.5, and 9 times longer than the runtime with 3000 samples, respectively). Moreover, considering the stabilization of the Markov chain, the initial samples must be discarded before computing the statistics.

Therefore, in this study, the characterisation of model uncertainty using the hybrid MCMC simulation was based on the following: (i) prior knowledge determined using the simplified method, as presented in Table 2; (ii) a Markov chain length of 10000 samples; (iii) statistical estimates computed from the last 5000 samples of the Markov chain; (iv) an initial point equal to the values of μ_ε and σ_ε defined as prior knowledge; (v) Normal distribution for the jump function with standard deviation defined as $SD = SD_{adeq}$; and (vi) parameters for characterising model uncertainty defined based on 10 simulation runs.

Figure 1 presents the sample distributions of μ_ε and σ_ε for both analytical methods. The samples generated by the hybrid MCMC simulation move within the μ_ε and σ_ε space as expected for a multivariate normal distribution, confirming the model's satisfactory performance.

Figure 2 and Table 3 show the model uncertainty characterisation for the AASHTO and *K-Stiffness* methods obtained by hybrid MCMC simulation. Figure 2 shows the histograms and the corresponding normal distribution curves of μ_ε and σ_ε, while Table 3 reports the parameters of the posterior normal distribution.

As expected, the *K-stiffness* method provides more accurate predictions compared to the AASHTO method. This is primarily because the *K-stiffness* method was developed and calibrated using monitoring data from real full-scale structures. In contrast, the AASHTO method is based on limit equilibrium theory and neglects several important factors, such as geosynthetic stiffness, facing stiffness, and the effects of soil compaction.

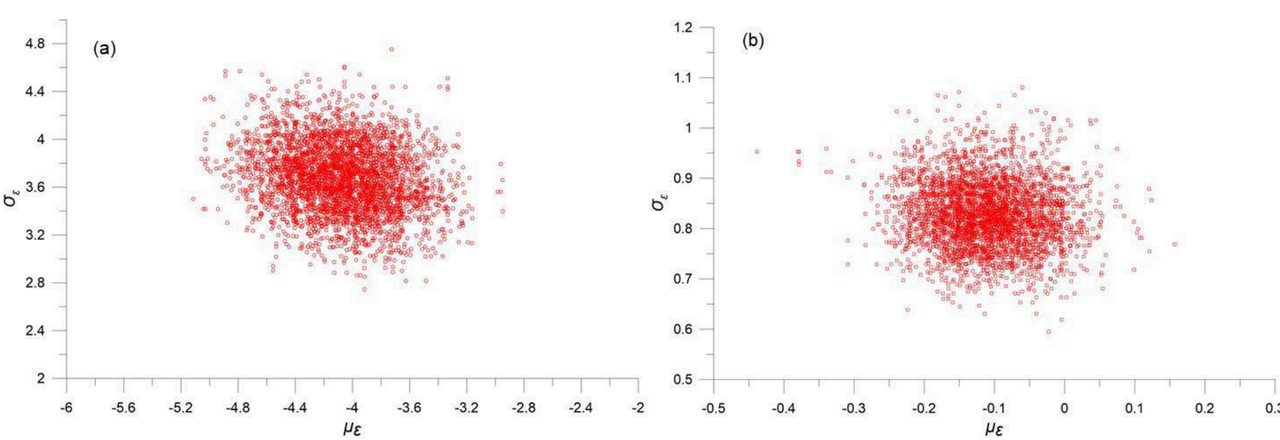

Figure 1. Sample distribution of μ_ε and σ_ε for (a) AASHTO method and (b) *K-stiffness method.*

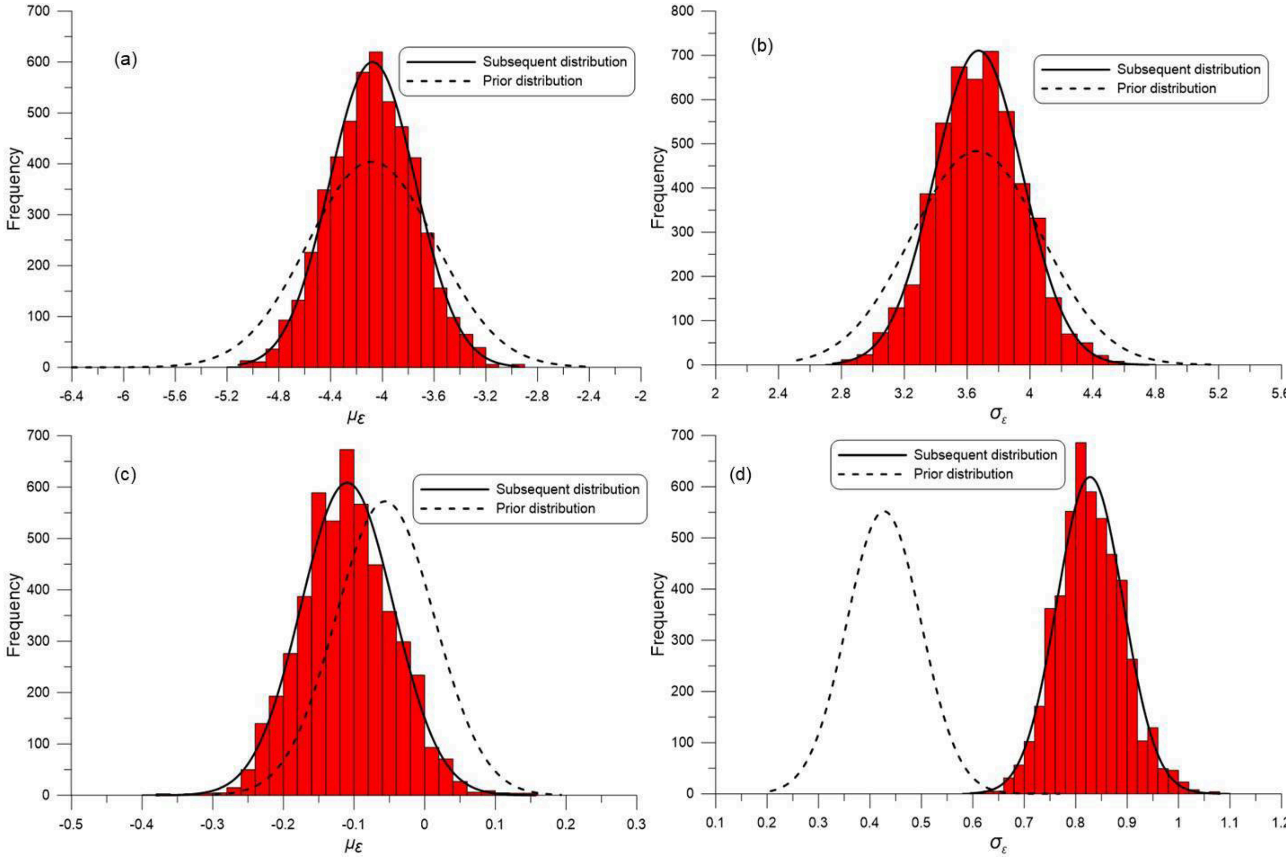

Figure 2. Histogram of μ_ε and σ_ε for (a-b) AASHTO method and (c-d) *K-stiffness* method. The dashed line represents the prior probability density function estimated by the simplified method and the solid line the best fits the samples generated by the hybrid MCMC simulation.

Table 3. Parameters of the posterior distribution of ε.

Design method	Dist.	μ_ε		σ_ε	
		Mean	*SD*	Mean	*SD*
AASHTO	Normal	-4.07	0.34	3.67	0.28
K-stiffness	Normal	-0.12	0.07	0.82	0.07

4. Conclusion

Overall, the simulations demonstrated good convergence and stability of the algorithms. In the tests carried out, the simulations were consistent with each other and showed a low coefficient of variation. In addition, the samples generated are consistent with the multivariate normal distribution. The choice of initial point did not significantly affect convergence; however, algorithm performance was found to be sensitive to the chain length and the tuning of the jump function.

Differences in the model uncertainty statistics were observed when comparing the simplified approach (Zhang et al., 2009) with the hybrid MCMC simulation approach (Zhang et al., 2012); however, considering the ease of implementation and the savings in computational time, the results of the approximate method were deemed satisfactory for an initial estimate. In this study, the simplified approach was employed to calibrate the model parameters (starting point, Markov chain size, jump function, and distribution type), and its results were used as prior knowledge in the subsequent analyses with the hybrid MCMC simulation approach.

Despite the satisfactory performance of the proposed framework, some limitations should be acknowledged. The robustness of the model uncertainty characterization is influenced by the amount and quality of available full-scale monitoring data, which naturally constrains the statistical confidence of the results. In the proposed probabilistic framework, soil parameters were assumed to be statistically independent, although for cohesionless backfills, positive correlations are often observed in practice.

Furthermore, in this study, the uncertainty associated with measurement data was neglected due to the lack of detailed information on instrumentation accuracy, which may slightly bias the results by attributing all discrepancies to model error.

Finally, the findings of this study demonstrate that the proposed probabilistic framework provides a robust methodology for characterising model uncertainty in geosynthetic-reinforced soil walls. The simplified approach offers an efficient and practical preliminary assessment, whereas the hybrid MCMC simulation enables a more accurate quantification of uncertainty. Overall, this framework can serve as a valuable tool for reliability-based design and informed engineering decision-making, supporting safer geotechnical designs.

Acknowledgements

The authors would like to acknowledge the support provided by the Coordination of Improvement of Higher Education Personnel (CAPES) and Geosynthetic Laboratory of the São Carlos School of Engineering – University of São Paulo (USP).

Declaration of interest

The authors have no conflicts of interest to declare. All co-authors have observed and affirmed the contents of the paper and there is no financial interest to report.

Authors' contributions

Marcell Gustavo Chagas Santos: Conceptualization, Data curation, Visualization, Methodology, Software, Writing – original draft. Jefferson Lins da Silva: Conceptualization, Supervision, Project administration, Validation, Writing – review & editing. Gabriel da Silva Silverio: Formal Analysis, Investigation, Resources, Writing – original draft. Bryan Robin Sanchez Ramirez: Formal Analysis, Resources, Writing – review & editing.

Data availability

The datasets generated analyzed in the course of the current study are available from the corresponding author upon request.

Declaration of use of generative artificial intelligence

This work was prepared with the assistance of generative artificial intelligence (GenAI) ChatGPT with the aim of improving the text previously written by the authors. The entire process of using this tool was supervised, reviewed and when necessary edited by the authors. The authors assume full responsibility for the content of the publication that involved the aid of GenAI.

List of symbols and abbreviations

d	observed response of geotechnical system
f	probability density function to normal distribution
g	model used to predict the behavior of a geotechnical system
k	normalization constant to make the probability density function valid
n	number of geotechnical systems
x	vector of random variables comprising model parameters and observation uncertainty
y	real response of geotechnical system
AASHTO	Association of State Highway and Transportation Officials
CAPES	Coordination of Improvement of Higher Education Personnel
COV	covariance of a variable
$G_{(x)}$	model prediction considering observation error
GW	geosynthetic wall
HDPE	high-density polyethylene
L	Likelihood function
MCMC	Monte Carlo sampling method via Markov chain
PEAD	high-Density Polyethylene.
PET	polyester
PP	polypropylene
SD	standard deviation
SD_{adeq}	standard deviation of the jump function
$S_{(x_i)}$	space of x_i
USP	University of São Paulo
X	set of input vectors representing model parameters for the n observations
γ	specific weight
Δ	observation uncertainty factor
ε	correction factor of geotechnical system
θ	vector of uncertain input parameters
μ	mean value of the distribution
σ	standard deviation of the distribution
$\{\mu_\varepsilon^0, \sigma_\varepsilon^0\}$	fixed initial point
ϕ	friction angle

References

American Association of State Highway and Transportation Officials – AASHTO. (2014). *AASHTO LRFD Bridge Design Specifications*. AASHTO.

Allen, T.M., Bathurst, R.J., & Berg, R.R. (2002). Global level of safety and performance of geosynthetic walls: an historical perspective. *Geosynthetics International*, 9(5-6), 395-450. https://doi.org/10.1680/gein.9.0224.

Allen, T.M., Christopher, B.R., & Holtz, R.D. (1992). Performance of a 12.6 m high geotextile wall in Seattle, Washington. In *Proceedings of the International*

Symposium on Geosynthetic-Reinforced Soil Retaining Walls (pp. 81-100), Denver, Colorado. Austin: International Geosynthetics Society.

Assis, H.B., & Nogueira, C.G. (2023). Comparative study of deterministic and probabilistic critical slip surfaces applied to slope stability using limit equilibrium methods and the First-Order Reliability Method. *Soils and Rocks*, 46(2), e2023013522. https://doi.org/10.28927/SR.2023.013522.

Basha, B.M., & Babu, G.L.S. (2010). Optimum design for external seismic stability of geosynthetic reinforced soil walls: reliability based approach. *Journal of Geotechnical and Geoenvironmental Engineering*, 136(6), 797-812. https://doi.org/10.1061/(ASCE)GT.1943-5606.0000289.

Basha, B.M., & Babu, G.L.S. (2012). Target reliability-based optimization for internal seismic stability of reinforced soil structures. *Geotechnique*, 62(1), 55-68. https://doi.org/10.1680/geot.8.P.076.

Bathurst, R.J., Simac, M.R., Christopher, B.R., & Bonczkiewicz, C.A. (1993). A database of results from a geosynthetic reinforced modular block soil retaining wall. In *International Symposium on Soil Reinforcement: Full Scale Experiments of the 80s* (pp. 341-365), Paris, France. London: ISSMGE.

Belo, J.L.P., Queiroz, P.I.B., & Lins da Silva, J. (2022). Geostatistical-based enhancement of RFEM regarding reproduction of spatial correlation structures and conditional simulations. *Soils and Rocks*, 45(4), 1-14. https://doi.org/10.28927/SR.2022.076121.

Bright, D.G., Collin, J.G., & Berg, R.R. (1994). Durability of geosynthetic soil reinforcement elements in Tanque Verde retaining wall structures. *Transportation Research Record: Journal of the Transportation Research Board*, (1439), 46-54.

Carrubba, P., Moraci, N., & Montanelli, F. (1999). Instrumented soil reinforced retaining wall: analysis of measurements. *Proceedings of Geosynthetics '99*, 2, 921-934.

Cetin, K.O., Kiureghian, A.D., & Seed, R.B. (2002). Probabilistic models for the initiation of seismic soil liquefaction. *Structural Safety*, 24(1), 67-82. https://doi.org/10.1016/S0167-4730(02)00036-X.

Christian, J.T., Ladd, C.C., & Baecher, G.B. (1994). Reliability applied to slope stability analysis. *Journal of Geotechnical Engineering*, 120(12), 2180-2207. https://doi.org/10.1061/(ASCE)0733-9410(1994)120:12(2180).

Christopher, B.R. (1993). *Deformation response and wall stiffness in relation to reinforced soil wall design* [Doctoral thesis]. Purdue University.

Dithinde, M., Phoon, K.K., Wet, M., & Retief, J.V. (2011). Characterization of model uncertainty in the static pile design formula. *Journal of Geotechnical and Geoenvironmental Engineering*, 137(1), 70-85. https://doi.org/10.1061/(ASCE)GT.1943-5606.0000401.

Duncan, J.M. (2000). Factors of safety and reliability in geotechnical engineering. *Journal of Geotechnical and Geoenvironmental Engineering*, 126(4), 307-316. https://doi.org/10.1061/(ASCE)1090-0241(2000)126:4(307).

Fannin, R.J., & Hermann, S. (1990). Performance data for a sloped reinforced soil wall. *Canadian Geotechnical Journal*, 27(5), 676-686. https://doi.org/10.1139/t90-080.

Ferreira, F.B., Topa Gomes, A., Vieira, C.S., & Lopes, M.L. (2016). Reliability analysis of geosynthetic-reinforced steep slopes. *Geosynthetics International*, 23(4), 301-315. https://doi.org/10.1680/jgein.15.00057.

Gelman, B.A., Carlin, B.P., Stern, H.S., Dunson, D.B., Vehtari, A., & Rubin, D.B. (2014). *Bayesian data analysis*. Chapman & Hall.

Geman, S., & Geman, D. (1984). Stochastic relaxation, Gibbs distributions, and the Bayesian restoration of images. *IEEE Transactions on Pattern Analysis and Machine Intelligence*, 6(6), 721-741. https://doi.org/10.1109/TPAMI.1984.4767596.

Gilbert, R.B., & Tang, W.H. (1995). Model uncertainty in offshore geotechnical reliability. In *Proceedings of the 27th Offshore Technology Conference* (pp. 557-567), Houston, Texas. Houston: OTC. https://doi.org/10.4043/7757-MS.

Heidarie Golafzani, S., Jamshidi Chenari, R., & Eslami, A. (2020). Reliability based assessment of axial pile bearing capacity: static analysis, SPT and CPT-based methods. *Georisk*, 14(3), 216-230. https://doi.org/10.1080/17499518.2019.1628281.

Hosseinpour, V., Saeidi, A., Salsabili, M., Nastev, M., & Nollet, M.-J. (2024). Development of a probabilistic seismic microzonation software considering geological and geotechnical uncertainties. *Georisk*, 18(3), 727-747. https://doi.org/10.1080/17499518.2024.2302183.

Juang, C.H., Yang, S.H., Yuan, H., & Khor, H. (2004). Characterization of the uncertainty of the Robertson and Wride model for liquefaction potential evaluation. *Soil Dynamics and Earthquake Engineering*, 24(9-10), 771-780. https://doi.org/10.1016/j.soildyn.2004.06.002.

Khademian, A., Abdollahipour, H., Bagherpour, R., & Faramarzi, L. (2017). Model uncertainty of various settlement estimation methods in shallow tunnels excavation; case study: qom subway tunnel. *Journal of African Earth Sciences*, 134, 658-664. https://doi.org/10.1016/j.jafrearsci.2017.08.003.

Knight, M.A., & Valsangkar, A.J. (1993). Instrumentation and performance of tilt-up panel wall. *Proceedings of Geosynthetics '93*, 30, 123-136.

Lacasse, S., & Nadim, F. (1996). Uncertainties in characterizing soil properties. In American Society of Civil Engineeers – ASCE (Ed.), *Uncertainty in the Geologic Environment: From theory to practice* (pp. 49-75). ASCE.

Mahmood, Z., Qureshi, M.U., Memon, Z.A., & Latif, Q.B.I. (2022). Ultimate limit state reliability-based optimization of MSE wall considering external stability. *Sustainability*, 14(9), 4968-4984. https://doi.org/10.3390/su14094968.

Metropolis, N., Rosenbluth, A.W., Rosenbluth, M.N., Teller, A.H., & Teller, E. (1953). Equation of state calculations by fast computing machines. *The Journal of Chemical Physics*, 21(6), 1087-1092. https://doi.org/10.1063/1.1699114.

Miyata, Y., & Bathurst, R.J. (2007). Evaluation of K-stiffness method for vertical geosynthetic reinforced granular soil walls in Japan. *Soil and Foundation*, 47(2), 319-335. https://doi.org/10.3208/sandf.47.319.

Moss, R.E., Seed, R.B., Kayen, R.E., Steward, J.P., & Kiureghian, A.D. (2006). CPT-based probabilistic and deterministic assessment of in situ seismic soil liquefaction potential. *Journal of Geotechnical and Geoenvironmental Engineering*, 132(8), 1032-1051. https://doi.org/10.1061/(ASCE)1090-0241(2006)132:8(1032).

Phoon, K.K., & Kulhawy, F.H. (2005). Characterization of model uncertainties for laterally loaded rigid drilled shafts. *Geotechnique*, 55(1), 45-54. https://doi.org/10.1680/geot.2005.55.1.45.

Santos, M.G.C., Lins da Silva, J., & Beck, A.T. (2018). Reliability-based design optimization of geosynthetic-reinforced soil walls. *Geosynthetics International*, 25(4), 442-455. https://doi.org/10.1680/jgein.18.00028.

Santoso, A.M., Phoon, K.K., & Quek, S.T. (2011). Effects of soil spatial variability on rainfall-induced landslides. *Computers & Structures*, 89(11-12), 893-900. https://doi.org/10.1016/j.compstruc.2011.02.016.

Schlosser, F., Hoteit, N., & Price, D. (1993). Instrumented full scale Freyssisol-Websol reinforced wall. In Sociedad Internacional de Mecánica del Suelo y Cimentaciones (Ed.), *Soil Reinforcement: Full Scale Experiments of the 80s* (pp. 299-320). Ecole Nationale des Ponts et Chaussées.

Tajiri, N., Sasaki, H., Nishimura, J., Ochiai, Y., & Dobashi, K. (1996). Full-scale failure experiments of geotextile-reinforced soil walls with different facings. In *Proceedings of the 3th International Symposium on Earth Reinforcement* (pp. 525-530), Fukuoka, Japan. London: CRC Press.

Tang, C., & Phoon, K.K. (2019). Characterization of model uncertainty in predicting axial resistance of piles driven into clay. *Canadian Geotechnical Journal*, 56(8), 1098-1118. https://doi.org/10.1139/cgj-2018-0386.

Wang, Y., Cao, Z., & Au, S.K. (2010). Efficient Monte Carlo simulation of parameter sensitivity in probabilistic slope stability analysis. *Computers and Geotechnics*, 37(7-8), 1015-1022. https://doi.org/10.1016/j.compgeo.2010.08.010.

Zhang, J., Tang, W.H., Zhang, L.M., & Huang, H.W. (2012). Characterizing geotechnical model uncertainty by hybrid Markov Chain Monte Carlo simulation. *Computers and Geotechnics*, 43, 26-36. https://doi.org/10.1016/j.compgeo.2012.02.002.

Zhang, J., Zhang, L.M., & Tang, W.H. (2009). Bayesian framework for characterizing geotechnical model uncertainty. *Journal of Geotechnical and Geoenvironmental Engineering*, 135(7), 932-940. https://doi.org/10.1061/(ASCE)GT.1943-5606.0000018.

Zhang, L.L., Zhang, J., Zhang, L.M., & Tang, W.H. (2010). Back analysis of slope failure with Markov Chain Monte Carlo simulation. *Computers and Geotechnics*, 37(7-8), 1728-1736. https://doi.org/10.1016/j.compgeo.2010.07.009.